

Fabri-Perot spectral filter that preserves image

H. V. Sarkissian, B. Ya. Zeldovich

School of Optics / CREOL, University of Central Florida, 4000 Central Florida Blvd., Orlando FL 32816-2700
Phone (407) 823-6831, FAX (407) 823-6880, boris@creol.ucf.edu; hakob@creol.ucf.edu

Abstract: Special arrangement of confocal Fabri-Perot interferometer is suggested as a spectral filter, which preserves image. Post-paraxial approximation is developed for the modes. Number of resolvable image pixels is estimated based on corrections to the eigenfrequencies.

©2000 Optical Society of America

OCIS codes: (120.2440) Filters, (120.2330) Fabri-Perot

1. Introduction

In some cases of active illumination of the target, high-resolution spectral selection may be used for discrimination between targets moving with different velocities and of different chemical composition. Most monochromators and various spectrographs limit spatial and angular spread of input light, [1, 2], and thus distort image. Volume diffraction grating at normal incidence may be used for spectral selection. However, spectral resolution $\delta\nu$ (1/cm) is about $1/L$, i.e. limited by the longitudinal thickness L of the grating. Number of available image pixels $N_x*N_y \approx (\text{Area})*(\delta\theta/\lambda)^2$ is limited by the acceptance angle of the volume grating, $\delta\theta \approx 1/(2\pi L/\lambda)$, [3].

Fabri-Perot interferometers (FPI) yield better spectral resolution, $\delta\nu \approx (2 - |r_1|^2 - |r_2|^2) / L$, [1]. FPI with flat mirrors trades angle to the wavelength and thus distorts image. Pierre Connes suggested in 1956 using Fabri-Perot interferometer with spherical mirrors, whose foci are coincident, for the spectral selection of broad area and angles of input radiation, [3]. However, the image is also scrambled by confocal FPI (CFPI).

We suggest here an arrangement of CFPI, which yields high spectral selectivity and preserving the image.

2. Layout of the suggested device

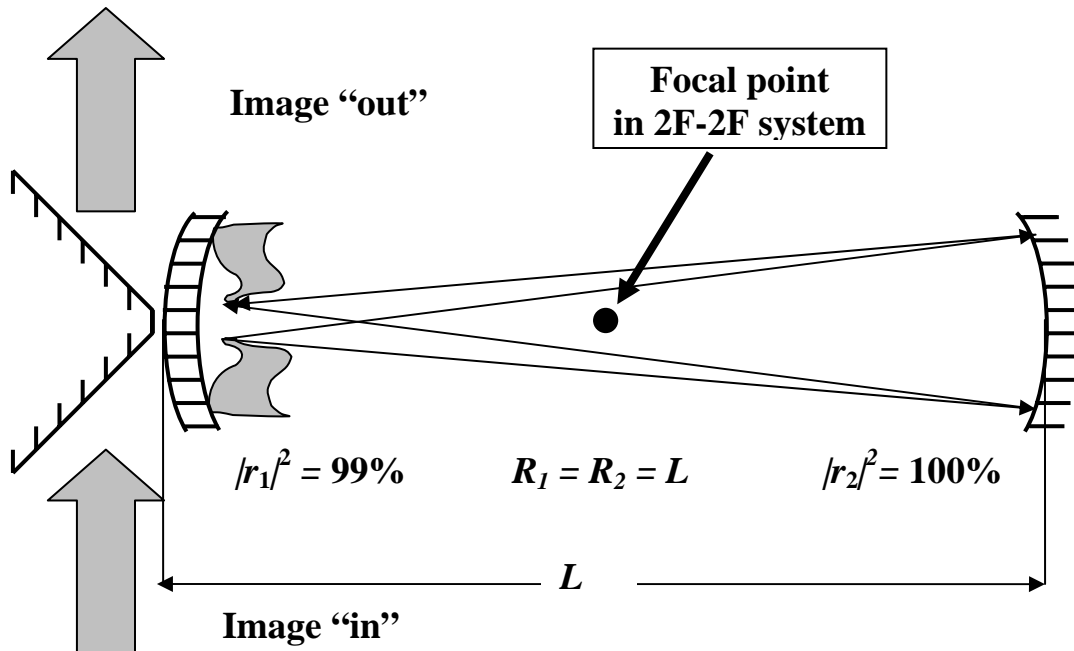


Fig. 1. This confocal FPI has highly reflective input/output mirror and 100% back mirror.

Input radiation illuminates the lower half of the first mirror. This light is imaged by the second mirror back to the upper half of the first mirror (2F-2F system!) From there spectrally filtered image is outputted.

3. Post-paraxial approximation for Gaussian beam and Hermit-Gaussian modes

Report Documentation Page

*Form Approved
OMB No. 0704-0188*

Public reporting burden for the collection of information is estimated to average 1 hour per response, including the time for reviewing instructions, searching existing data sources, gathering and maintaining the data needed, and completing and reviewing the collection of information. Send comments regarding this burden estimate or any other aspect of this collection of information, including suggestions for reducing this burden, to Washington Headquarters Services, Directorate for Information Operations and Reports, 1215 Jefferson Davis Highway, Suite 1204, Arlington VA 22202-4302. Respondents should be aware that notwithstanding any other provision of law, no person shall be subject to a penalty for failing to comply with a collection of information if it does not display a currently valid OMB control number.

1. REPORT DATE 10 AUG 2004	2. REPORT TYPE N/A	3. DATES COVERED -			
4. TITLE AND SUBTITLE Fabri-Perot spectral filter that preserves image		5a. CONTRACT NUMBER			
		5b. GRANT NUMBER			
		5c. PROGRAM ELEMENT NUMBER			
6. AUTHOR(S)		5d. PROJECT NUMBER			
		5e. TASK NUMBER			
		5f. WORK UNIT NUMBER			
7. PERFORMING ORGANIZATION NAME(S) AND ADDRESS(ES) School of Optics / CREOL, University of Central Florida, 4000 Central Florida Blvd., Orlando FL 32816-2700		8. PERFORMING ORGANIZATION REPORT NUMBER			
9. SPONSORING/MONITORING AGENCY NAME(S) AND ADDRESS(ES)		10. SPONSOR/MONITOR'S ACRONYM(S)			
		11. SPONSOR/MONITOR'S REPORT NUMBER(S)			
12. DISTRIBUTION/AVAILABILITY STATEMENT Approved for public release, distribution unlimited					
13. SUPPLEMENTARY NOTES See also ADM001691, Phase Conjugation for High Energy Lasers.					
14. ABSTRACT					
15. SUBJECT TERMS					
16. SECURITY CLASSIFICATION OF:			17. LIMITATION OF ABSTRACT UU	18. NUMBER OF PAGES 3	19a. NAME OF RESPONSIBLE PERSON
a. REPORT unclassified	b. ABSTRACT unclassified	c. THIS PAGE unclassified			

Number of undistorted image pixels equals half of the modes' number, which possess eigenfrequencies within CFPI's linewidth Γ . Since eigenfrequencies are coincident within the paraxial approximation, we explore post-paraxial corrections, both in the solutions of Helmholtz equation,

$$(\nabla \cdot \nabla + k^2)E(x, y, z) = 0, \quad k = 2\pi / \lambda, \quad (1)$$

and in the boundary conditions at the mirrors. We use these notations:

$$R_1 = R_2 = L, \quad z_0 = L/2, \quad a = \sqrt{z_0/k} \equiv \sqrt{L\lambda/4\pi} \equiv W_0/\sqrt{2}, \quad kz_0 \equiv kL/2; \quad (2)$$

z_0 , waist length (HWHM), a , waist width (HWe⁻¹M); $W_0 =$ (HWe⁻²M). A relevant exact solution of Helmholtz equation is

$$E(x, y, z) = \frac{\exp(ikR_{\text{compl}})}{R_{\text{compl}}}, \quad R_{\text{compl}} = \sqrt{(z - iz_0)^2 + \rho^2}, \quad \rho^2 = x^2 + y^2 \quad (3)$$

This solution is a good start to describe paraxial Gaussian beam. It possesses singularity at $z = 0, \rho = z_0$, i.e. at large distance from the work space of this FPI. We use the expansion of the beam (3) up to corrections $\approx (\rho/a)^4/(kL)$ including:

$$G_{00}(x, y, z) = \frac{1}{1 + i(z/z_0) - \rho^2/[2a^2kz_0(1 + i(z/z_0))]} \cdot \exp\left\{ ikz - \frac{\rho^2}{2a^2[1 + i(z/z_0)]} - \frac{\rho^4}{8a^4[1 + i(z/z_0)]^3 kz_0} \right\} \quad (4)$$

This should be accompanied by the mirrors' shape equation:

$$z_{\text{mirror}}(\rho) \approx \pm \left[z_0 - \frac{\rho^2}{4z_0^2} - \mu \frac{\rho^4}{z_0^4} \right], \quad (5)$$

$\mu = (1/16)$ for spherical mirrors. Envelope of the paraxial Gaussian beam has constant phase at the mirrors (also considered in paraxial approximation); phase is constant for Hermit-Gaussian modes as well, so that

$$\omega_{m,p,q} = ck_{m,p,q} = \frac{c}{2L} (2\pi m + \pi(p + q + 1)) - i\Gamma + c\delta k_{m,p,q}. \quad (6)$$

Deviation $\delta\psi(x,y)$ of the phase at the mirror's surface, as it happens in post-paraxial approximation, leads to eigenfrequency correction,

$$M_{m,p,q}(z(\rho), x, y) = \pm |M_{m,p,q}(z(\rho), x, y)| \exp[i\delta\psi(x, y)], \quad (7)$$

$$\delta k_{m,p,q} = - \left[\iint \delta\psi(x, y) \cdot |M_{m,p,q}(z(\rho), x, y)|^2 dx dy \right] / \left[\iiint |M_{m,p,q}(x, y, z)|^2 dx dy dz \right]. \quad (8)$$

Higher Hermit-Gaussian beams may be obtained via generating function:

$$F(u, w) \cdot G_{00}(x - u, y - w, z) = \sum_{p=0}^{\infty} \sum_{q=0}^{\infty} (u)^p (w)^q M_{p,q}(x, y, z); \quad F(u, w) = \exp[(u^2 + w^2)/4a^2] \quad (9)$$

Lengthy calculations based on (6-9) result in limitation on the modes' transverse indexes p, q , for which the condition $\delta\omega < \Gamma$ is satisfied:

$$|c\delta k_{m,p,q}| \leq \Gamma, \quad \Gamma \approx (2 - |r_1|^2 - |r_2|^2) \cdot (c/4L), \quad N = \frac{1}{2} \delta p \cdot \delta q \approx \frac{4}{3} \cdot \frac{L}{\lambda} \cdot (2 - |r_1|^2 - |r_2|^2) \quad (10)$$

This estimation was done for purely spherical mirrors; it constitutes the main result of this work.

Note that an ellipsoidal shape of the mirrors exists, which exactly coincides with the wavefront of Helmholtz equation's exact solution (3):

$$\text{Re}[R_{\text{compl}}(x, y, z)] = 0 \rightarrow \left(\frac{z}{z_0} \right)^2 + \left(\frac{\rho}{z_0 \sqrt{2}} \right)^2 = 1, \quad (11)$$

and here $\mu = +(1/32)$.

Numerical estimation for $L=1$ m, $\lambda=500$ nm, $(2-|r_1|^2 - |r_2|^2)=0.01$ yields $N \approx 30,000$.

4. References

1. E. Hecht, Optics, 3rd Edition, Addison-Wesley , Reading, MA (1998).
2. M. Born, E. Wolf, Principles of Optics, 7-th ed., Cambridge University Press (1999).
3. B. Zeldovich, A. Mamaev, V. Shkunov, Speckle-wave interactions and holography, CRC Press, Boca Raton (1995)
4. P. Connes (1956), cited from [1], page 418.